

# Tailoring the transmission lineshape spectrum of zigzag graphene nanoribbon based heterojunctions via controlling its width and edge protrusions

K. P. Dou,<sup>a</sup> X. X. Fu,<sup>a</sup> Abir De Sarkar<sup>b</sup> and R. Q. Zhang<sup>\*a</sup>

<sup>a</sup> Department of Physics and Materials Science, City University of Hong Kong, Hong Kong SAR

<sup>b</sup> Computational Nanoscience Group, Institute of Nano Science and Technology (An Autonomous Institute supported by the Department of Science and Technology, Government of India), Habitat Centre, Phase X, Sector-64, Mohali, Punjab-160 062, India

\*Corresponding author. Email: aprqz@cityu.edu.hk

## Formation energy:

Take S11 as an example:

$$E_{\text{formation}} = E_{\text{S11}} - E_{\text{S10}} - 3E_{\text{Carbon}} - E_{\text{Hydrogen}}$$

where  $E_{\text{S11}}$  and  $E_{\text{S10}}$  are the total energies of S11 and S10, respectively.  $E_{\text{carbon}}$  and  $E_{\text{Hydrogen}}$  are the total energies of per carbon atom of graphene and per hydrogen atom of an isolated  $\text{H}_2$  molecule.

The formation energies for each model are: -0.735 eV (S11), -1.515 eV (S12), -0.483 eV (S21) and -1.249 eV (S22), respectively. In view of theoretical study on doped GNR system, the relative formation energy could be as high as 3 eV depending on dopant position.<sup>1</sup> In addition, the formation energy for dopant introduced near defect is more than -6 eV.<sup>2</sup> The theoretical value is meant as a qualitative guide rather than providing quantitative one to experimental work.

## Model fitting:

### (a) Fitting for S10

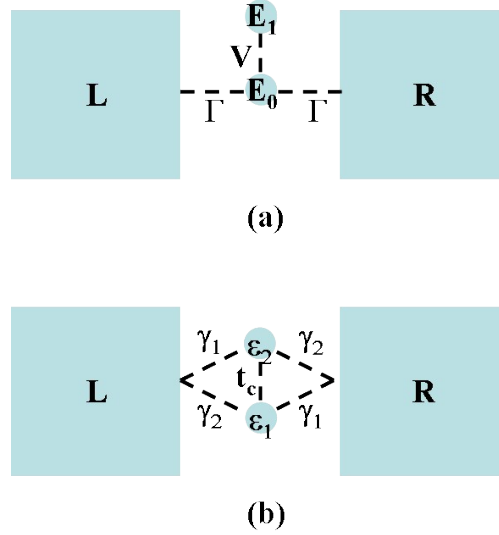


Figure S1 Two transport models for S10.

The typical Fano resonance model<sup>3,4</sup> assumes two energy levels,  $E_0$  and  $E_1$  (Figure S1(a)), with a weak coupling  $V$  between them.  $E_0$  is symmetrically coupled to left and right electrodes via the coupling constant  $\Gamma$  while  $E_1$  is strongly localized in the device region and uncoupled from the electrodes. The transmission can be expressed as Equation (1) in the content (Junctions with small width difference).

In addition, as shown in Figure S1(b), we use double dot model with parallel configuration<sup>6</sup> to fit for the transmission of S10:

$$T(E) = \frac{4[t_c \bar{\gamma} - \gamma_{12}(\varepsilon - \bar{\varepsilon})]^2}{[(\varepsilon - \bar{\varepsilon})^2 - (\Delta\varepsilon/2)^2 - t_c^2 - (\Delta\gamma)^2/4]^2 + 4[\bar{\gamma}(\varepsilon - \bar{\varepsilon}) - t_c \gamma_{12}]^2} \quad (S1)$$

with  $\bar{\varepsilon} = (\varepsilon_1 + \varepsilon_2)/2$ ,  $\Delta\varepsilon = \varepsilon_1 - \varepsilon_2$ ,  $\bar{\gamma} = (\gamma_1 + \gamma_2)/2$ ,  $\Delta\gamma = \gamma_1 - \gamma_2$ , and  $\gamma_{12} = \sqrt{\gamma_1 \gamma_2}$ .

According to S10,  $\gamma_1 = \gamma_2 = \gamma$ , the transmission takes the form:

$$T(E) = \frac{4\gamma^2}{[\varepsilon - \bar{\varepsilon} + t_c - (\Delta\varepsilon/2)^2 / (\varepsilon - \bar{\varepsilon} - t_c)]^2 + 4\gamma^2} \quad (S2)$$

With appropriate fitting parameters of  $\bar{\varepsilon} = -0.16$  eV,  $t_c = 0.133$  eV,  $\gamma = 0.28$  eV, and  $\Delta\varepsilon = -0.178$  eV, the double dot model again repeats the essential features of Fano resonance in S10, as shown in Figure S2. The values of  $|\Delta\varepsilon|$  and  $\gamma$  are of the same order. This fulfils the condition for Fano resonance given in reference 6. The energy level  $\varepsilon_1$  participates in the transmission while  $\varepsilon_2$  is localized. The two levels could be relevant with band 288 and band 290, respectively, as shown in Figure 3(a).

Both fitting procedures leads to the same feature and hence it is suitable to use Fano resonance to describe the transmission shape in S10.

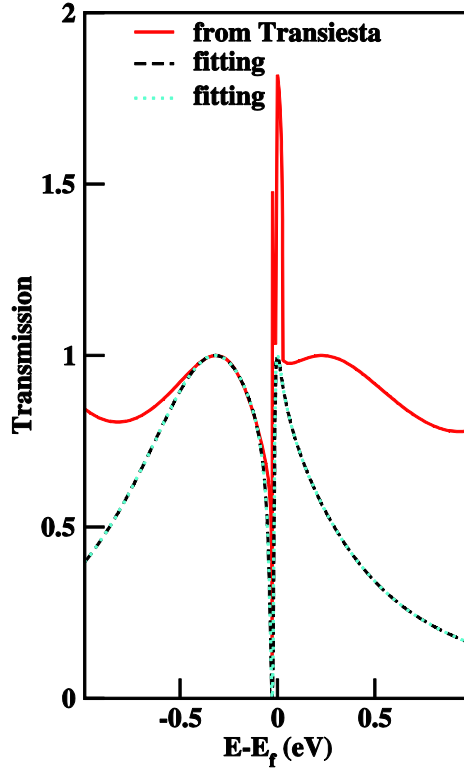


Figure S2 Transmission spectra of S10 with fitting curves: black dashed line from Figure S1(a) and cyan dashed line from Figure S1(b).

### (b) Fitting for S11, and S21

The transmission of S11, and S21 near  $E_f$  resonance can be fitted using the single-level model.<sup>3,4</sup> This model assumes a single conducting level at energy  $E_0$  coupled symmetrically to each lead via the coupling constant  $\Gamma$ . This yields a Lorentzian shaped peaks centred at the energy  $E_0$  in transmission:

$$T(E) = \frac{\Gamma^2}{(E - E_0)^2 + \Gamma^2} \quad (S3)$$

The model fitting parameters are  $E_0 = -0.02$  eV and  $\Gamma = 0.226$  eV for S11,  $E_0 = 0$  eV and  $\Gamma = 0.086$  eV for S21, respectively.

### (c) Fitting for S20

The transmission of S20 near  $E_f$  can be fitted using the two-level model, as shown in Figure. S3(a). This model assumes each conducting energy level is coupled symmetrically to electrodes via a coupling constant ( $\Gamma_1$  and  $\Gamma_2$ ) and contributes an independent channel for electron transport.<sup>3,5</sup>  $T(E)$  is thus a sum

of two Lorentzian shaped peaks centred at the energy of the conducting levels ( $E_1$  and  $E_2$ ).

$$T(E) = \frac{\Gamma_1^2}{(E - E_1)^2 + \Gamma_1^2} + \frac{\Gamma_2^2}{(E - E_2)^2 + \Gamma_2^2} \quad (S4)$$

The model fitting parameters are  $E_1 = -0.42$  eV,  $E_2 = 0.37$  eV,  $\Gamma_1 = 0.077$  eV, and  $\Gamma_2 = 0.086$  eV.

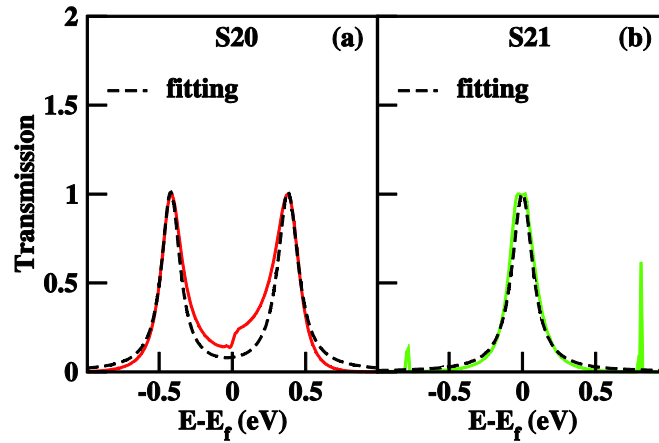


Figure S3 Transmission spectra of models S20 and S21 with fitted curves (black dashed line).

### Spin effect:

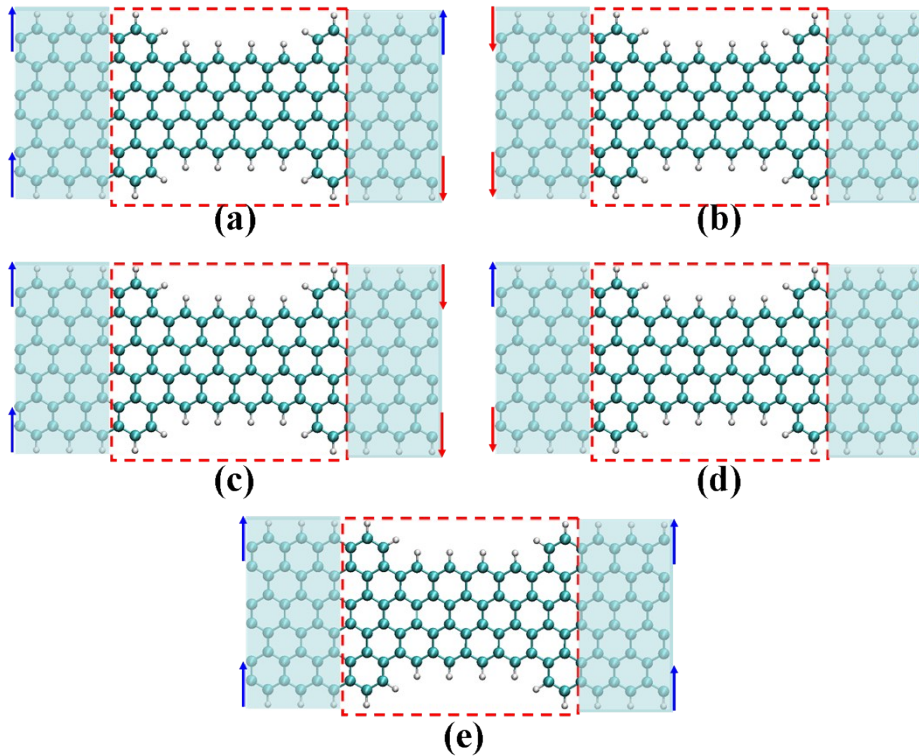


Figure S4 Schematic diagram of different spin configurations in model S10: (a)  $SC_{u0}$ (b)  $SC_{d0}$  (c)  $SC_{ud}$  (d)  $SC_{00}$  and (e)  $SC_{uu}$ . Spin up and down are marked by blue and red arrows.

To evaluate the dependence of transmission on spin effect, we perform spin calculations of models S10, S11 and S12. Different spin configurations are shown in Figure S4 with S10 as the examples:  $SC_{u0}$ ,  $SC_{d0}$ ,  $SC_{ud}$ ,  $SC_{00}$  and  $SC_{uu}$ . The transmission spectra are shown in Figure S5-S9. The results indicate that the spin configuration  $SC_{uu}$  is most efficient to break the spin degeneracy in all three junctions. These can be traced back to the band analysis in Figure S10-S14.

In view of one recent work on molecular spintronics, polyacetylene with donor/acceptor group is found to possess antiresonance dip near the Fermi level in the spin down /up transmission spectrum.<sup>7</sup> For comparison, both S10 and S11 with spin configuration  $SC_{uu}$  present antiresonance near the Fermi level in both spin up and down transmission. Thus the present work outline other possibility for exploiting spin application with destructive quantum interference effect in GNR based devices.

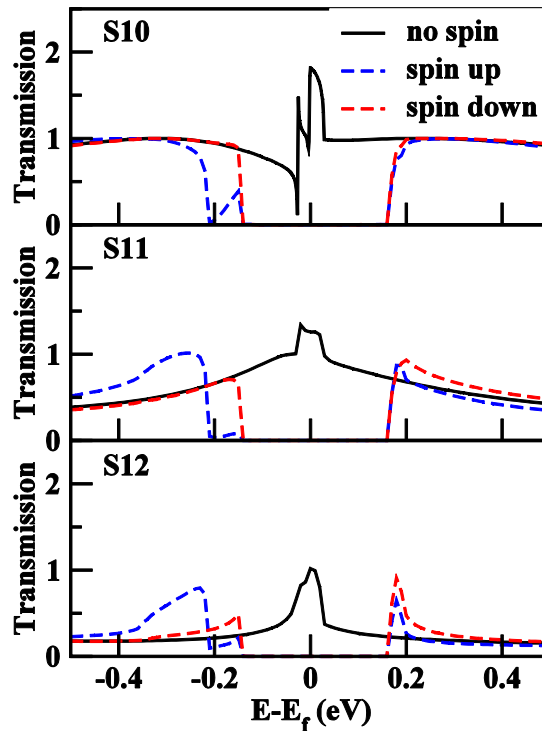


Figure S5 Transmission spectra of models S10, S11 and S12 with  $SC_{u0}$  configuration. Transmission spectra without spin effect are also present (black line).

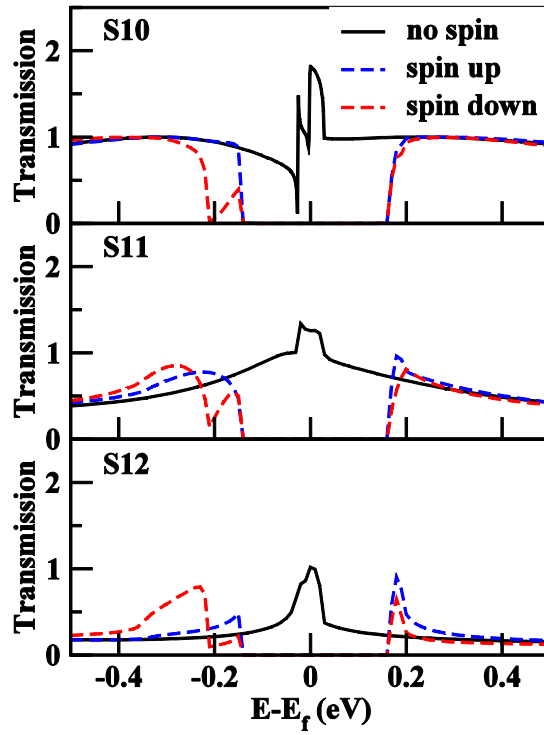


Figure S6 Transmission spectra of models S10, S11 and S12 with  $SC_{d0}$  configuration. Transmission spectra without spin effect are also present (black line).

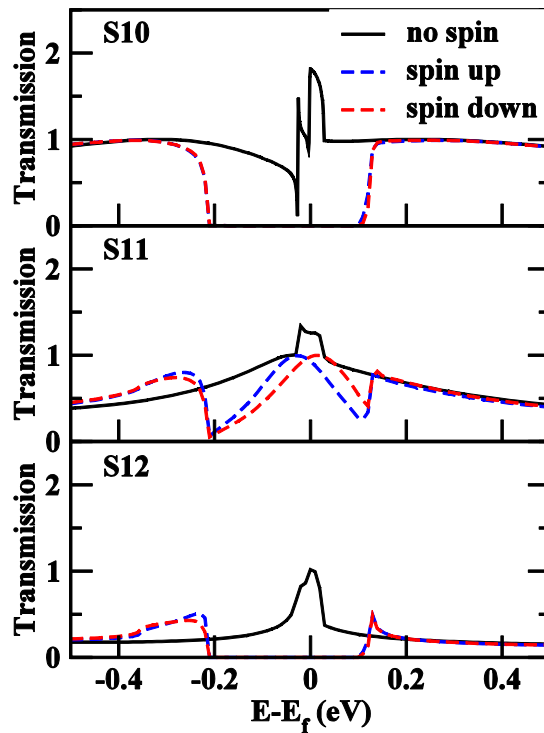


Figure S7 Transmission spectra of models S10, S11 and S12 with  $SC_{ud}$  configuration. Transmission spectra without spin effect are also present (black line).

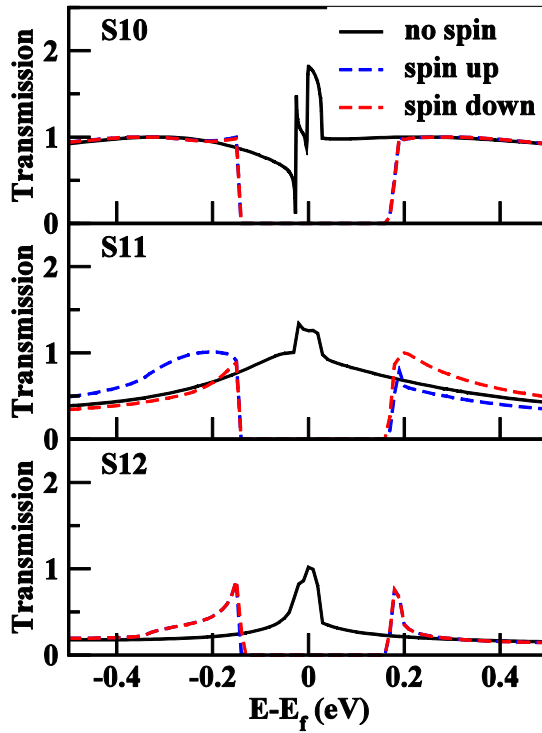


Figure S8 Transmission spectra of models S10, S11 and S12 with  $SC_{00}$  configuration. Transmission spectra without spin effect are also present (black line).

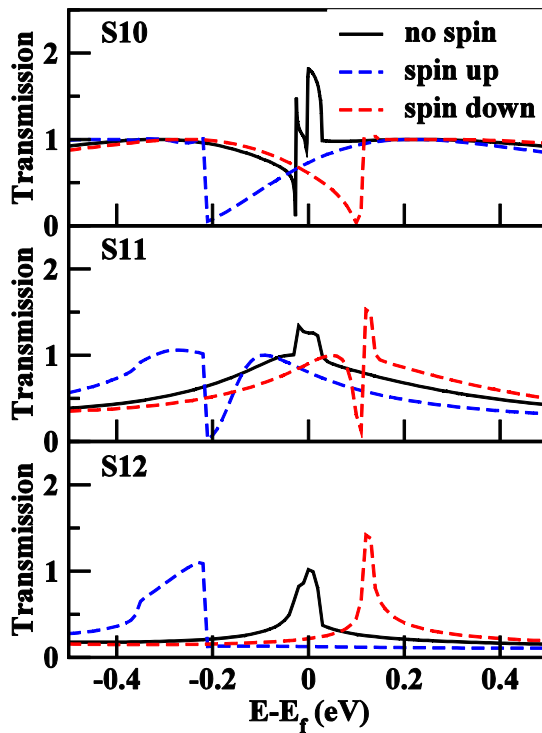


Figure S9 Transmission spectra of models S10, S11 and S12 with  $SC_{uu}$  configuration. Transmission spectra without spin effect are also present (black line).

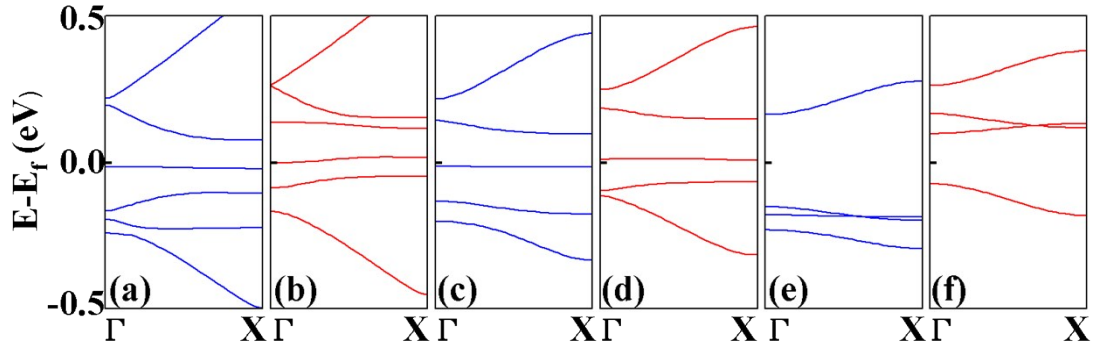


Figure S10 Electronic band structure under  $SC_{u0}$  configuration for S10 (a) and (b); S11(c) and (d); S12 (e) and (f), calculated upon assuming periodicity along the transport direction. Bands of spin up and down are shown in blue and red.

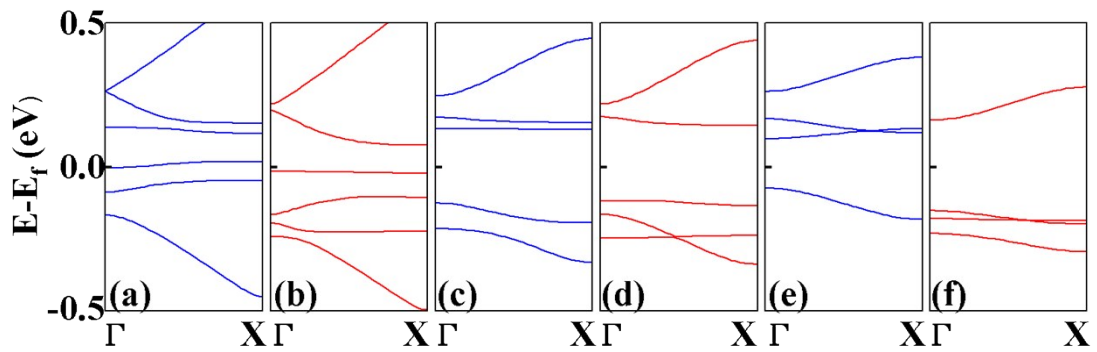


Figure S11 Electronic band structure under  $SC_{d0}$  configuration for S10 (a) and (b); S11(c) and (d); S12 (e) and (f), calculated upon assuming periodicity along the transport direction. Bands of spin up and down are shown in blue and red.

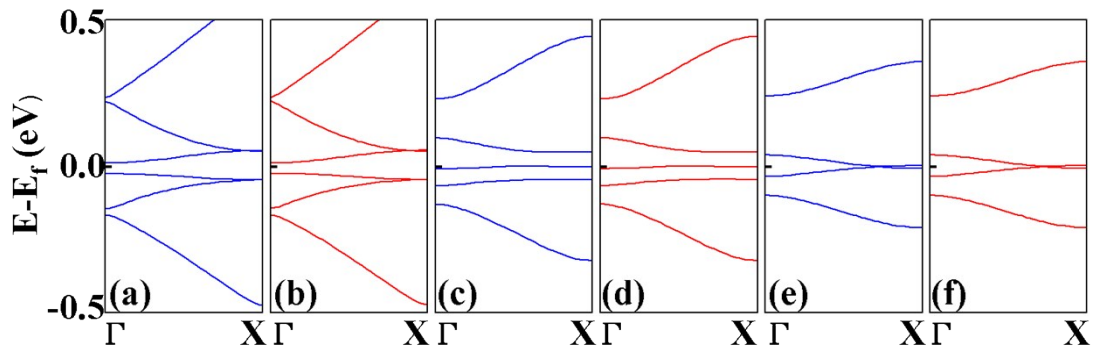


Figure S12 Electronic band structure under  $SC_{ud}$  configuration for S10 (a) and (b); S11(c) and (d); S12 (e) and (f), calculated upon assuming periodicity along the transport direction. Bands of spin up and down are shown in blue and red.

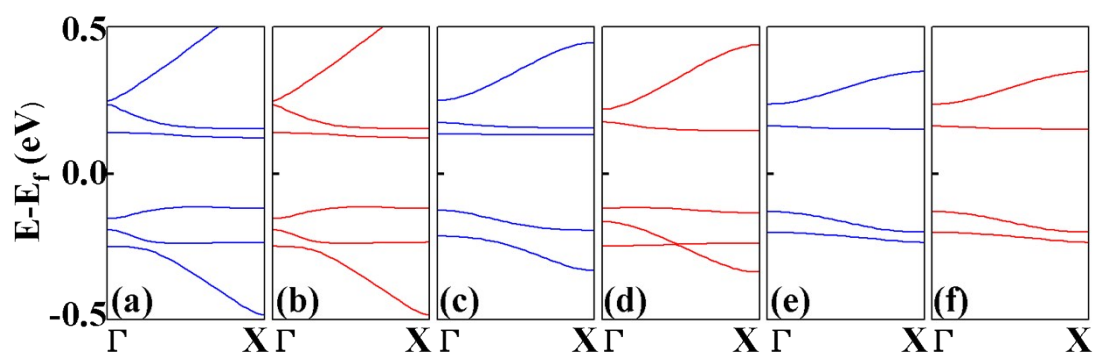


Figure S13 Electronic band structure under  $SC_{00}$  configuration for S10 (a) and (b); S11(c) and (d); S12 (e) and (f), calculated upon assuming periodicity along the transport direction. Bands of spin up and down are shown in blue and red.

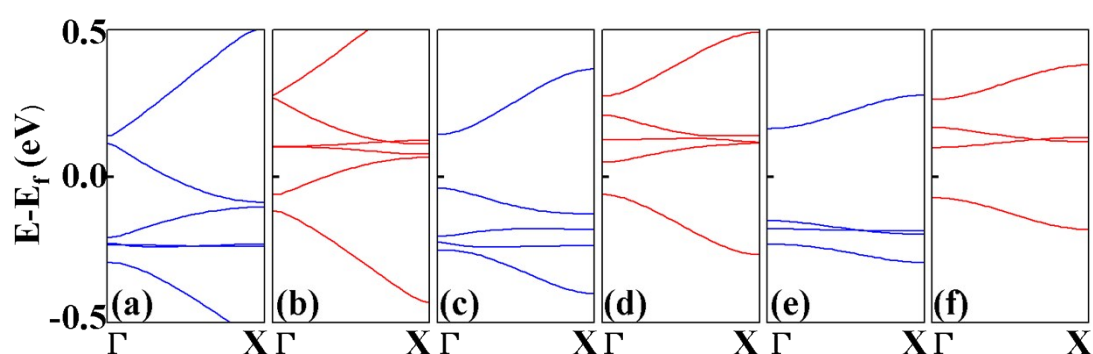


Figure S14 Electronic band structure under  $SC_{uu}$  configuration for S10 (a) and (b); S11(c) and (d); S12 (e) and (f), calculated upon assuming periodicity along the transport direction. Bands of spin up and down are shown in blue and red.

## References

- 1 E. Cruz-Silva, Z. M. Barnett, B. G. Sumpter, and V. Meunier, *Phys. Rev. B*, 2011, **83**, 155445.
- 2 R. Faccio, L. Fernández-Werner, H. Pardo, C. Goyenola, O. N. Ventura, and Á. W. Mombrú, *J. Phys. Chem. C*, 2010, **114**, 18961–18971.
- 3 C. J. Lambert, *Chem. Soc. Rev.*, 2015, **44**, 875-888.
- 4 J. C. Cuevas and E. Scheer, *Molecular Electronics: An Introduction to Theory and Experiment* World Scientific, Singapore, 1st ed, 2010.
- 5 T. Markussen, R. Stadler and K. S. Thygesen, *Phys. Chem. Chem. Phys.*, 2011, **13**, 14311-14317.
- 6 M. L. L. de Guevara, F. Claro and P. A. Orellana, *Phys. Rev. B*, 2003, **67**, 195335.
- 7 A. Saraiva-Souza, M. Smeu, L. Zhang, A. G. S. Filho, H. Guo and M. A. Rater, *J. Am. Chem. Soc.* 2014, **136**, 15065-15071.